Soft Science

# Supplementary Material: Injectable and tissue-conformable conductive hydrogel for MRI-compatible brain-interfacing electrodes

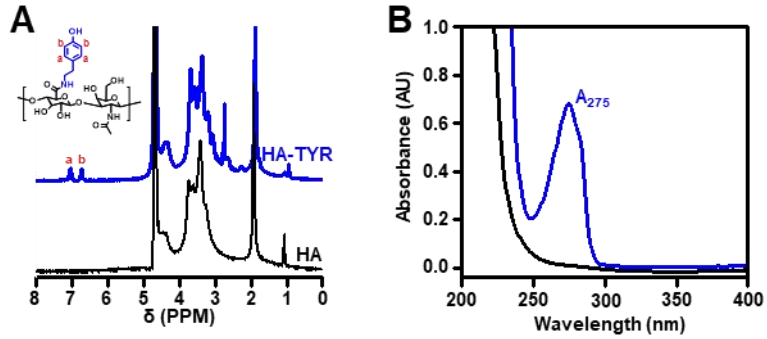


**Supplementary Figure 1. Synthesis of HATYR** (A) $^{1}$H-NMR spectroscopy of HATYR (blue) and HA (black). Differently marked peaks (red) represent hydrogen atoms in phenol of tyramine. (B) UV–Vis spectroscopy of HA (black) and HATYR (blue) at the absorbance peak of 275 nm (tyramine).

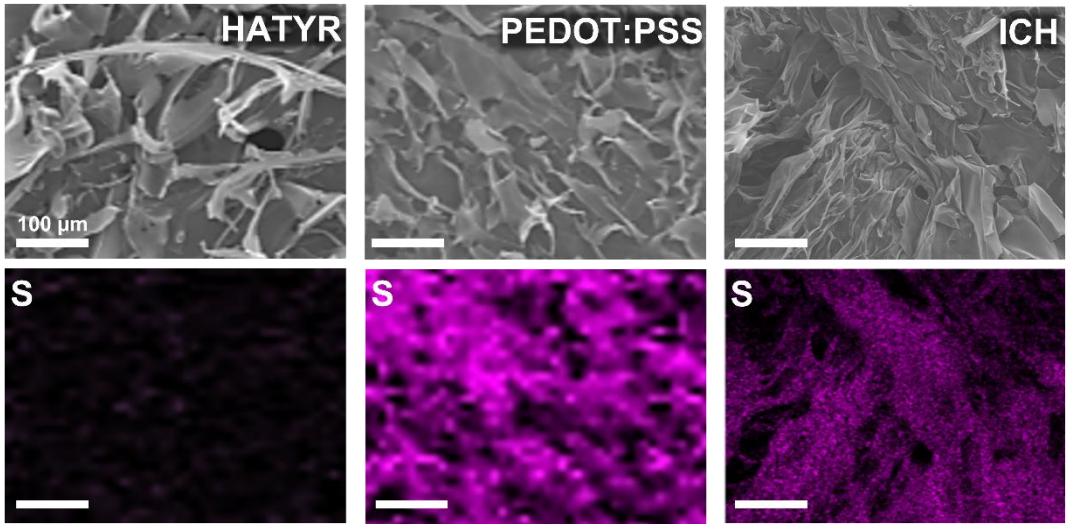


**Supplementary Figure 2. Scanning electron spectroscopy (SEM).** HATYR, PEDOT:PSS, and ICH are imaged under SEM with energy-dispersive X-ray spectroscopy of sulfur (S) elements below, respective to the above images. Scale bar: 100 μm.

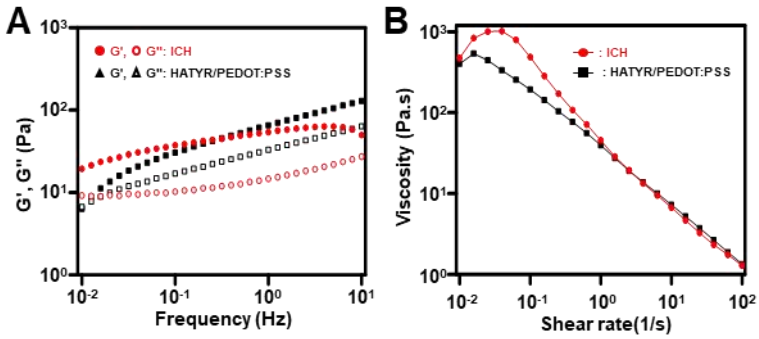


**Supplementary Figure 3. Viscoelastic properties of hydrogel formulations.** (A) Oscillation frequency sweep measurements of HATYR/PEDOT:PSS (black) and ICH (red). The filled circles represent the storage modulus (G'), and the empty circles represent the loss modulus (G"). (B) Viscosity with increasing shear rates (0.01–100 $s^{-1}$) of HATYR/PEDOT:PSS (black) and ICH (red).

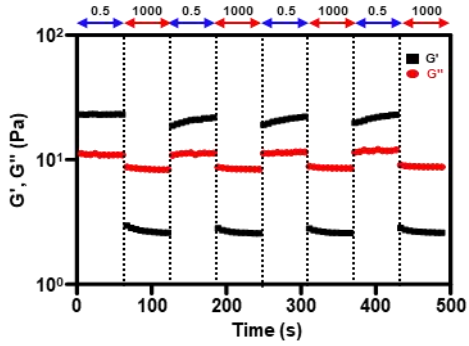


**Supplementary Figure 4. Self-healing properties of ICH.** Evaluation of disruption and recovery of storage (G') (black) and loss (G") (red) moduli of hydrogels depending on an alternating strain of 0.5% and 1000%.

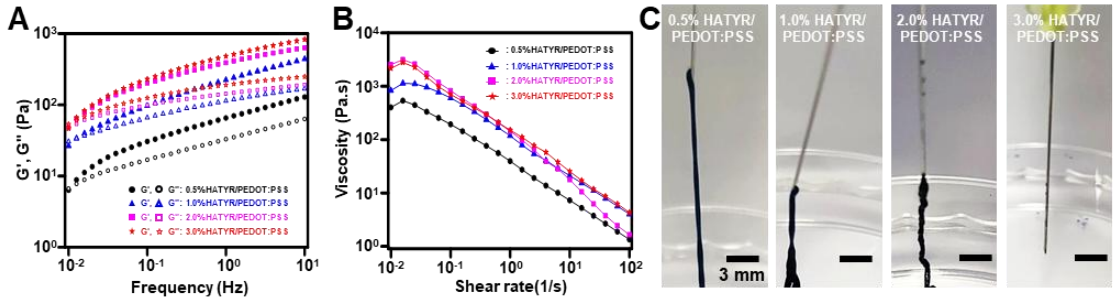


**Supplementary Figure 5. Injectability characterization of .** (A) Oscillation frequency sweep measurements of different concentration (0.5, 1, 2, and 3%) of HATYR at uniform concentration of PEDOT:PSS. The filled represent the storage modulus (G'), and the empty represent the loss modulus (G''). (B) Viscosity with increasing shear rates (0.01–100 $s^{-1}$) of different concentration (0.5, 1, 2, and 3%) of HATYR at uniform concentration of PEDOT:PSS. (C) Photographs of injectability different HATYR/PEDOT:PSS formulations in 30G needle. Scale bar: 3 mm.

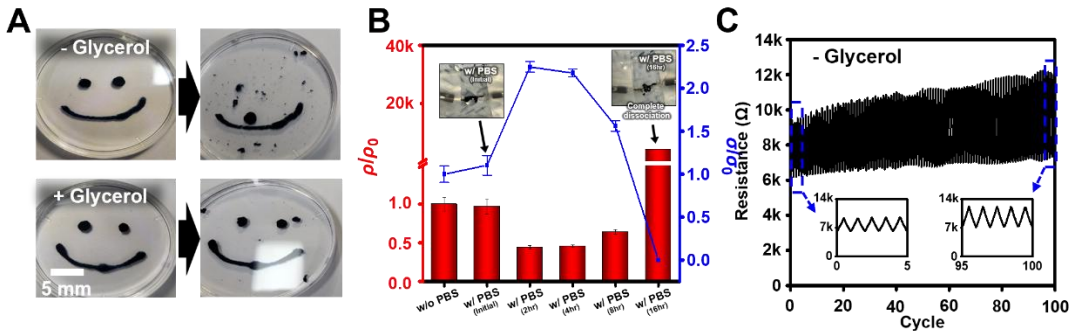


**Supplementary Figure 6. Properties from addition of glycerol.** (A) Photographs of changes in structure of injected ICH w/ and w/o glycerol before (left) and after (right) 30 min. (B) Normalized resistivity ($\Delta\rho/\rho_0$) and conductivity ($\Delta\sigma/\sigma_0$) of ICH while soaked in a PBS buffer from 0 hr to 16 hrs (inset photographs = soaked ICH in PBS buffer at 0 hr and 16 hrs). (C)Reversible electrical reliability of the ICH (-glycerol) during cyclic stretching/releasing tests (at a speed of 0.3 mm/s and strain of 100%) on one hundred times (inset images represent initial and final 5 peaks). Scale bar: 5 mm.

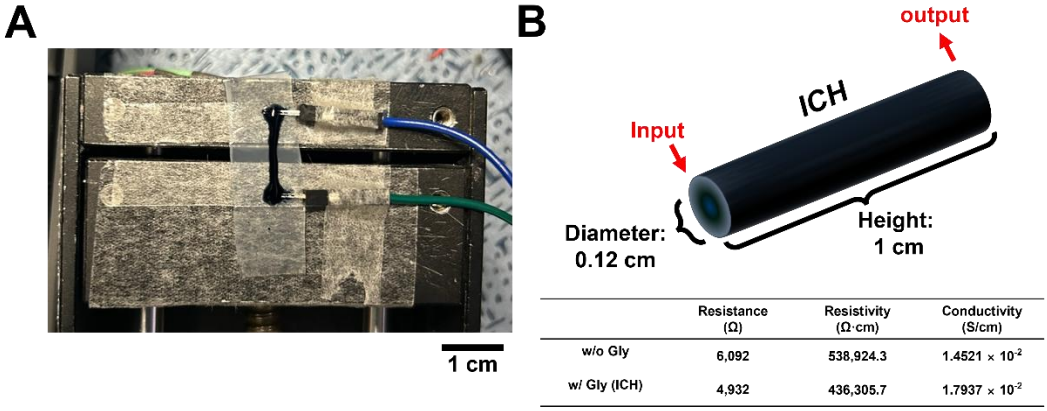


| | Resistance (Ω) | Resistivity (Ω·cm) | Conductivity (S/cm) |
|---|---|---|---|
| w/o Gly | 6,092 | 538,924.3 | $1.4521 \times 10^{-2}$ |
| w/ Gly (ICH) | 4,932 | 436,305.7 | $1.7937 \times 10^{-2}$ |

**Supplementary Figure 7**. (A) Sample photograph for electrical resistance measurements. (B) Conductivity calculation from initial resistance of 'w/o glycerol' and 'w/ glycerol (ICH)'.

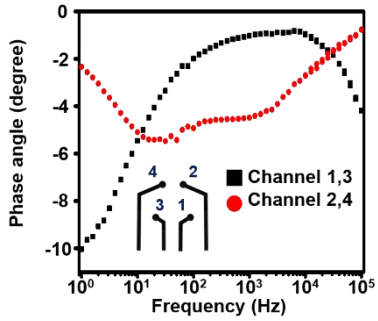


**Supplementary Figure 8**. Phase angle from impedance spectroscopy of different pair of channels (long trace from '1, 3' and short trace from '2, 4') from ICH-based soft brain interface in PBS solution.